Audio Engineering Society
Convention Express Paper 210

Presented at the 156th Convention
2024 June 15-17, Madrid, Spain

This Express Paper was selected on the basis of a submitted synopsis that has been peer-reviewed by at least two qualified anonymous reviewers. The complete manuscript was not peer reviewed. This Express Paper has been reproduced from the author's advance manuscript without editing, corrections or consideration by the Review Board. The AES takes no responsibility for the contents. This paper is available in the AES E-Library (http://www.aes.org/e-lib) all rights reserved. Reproduction of this paper, or any portion thereof, is not permitted without direct permission from the Journal of the Audio Engineering Society.

One design for reducing surround dip effect of loudspeaker responses

Jun Gu[1], Zhi Li[2], and Jianbin Yang[3]

[1] *Dynaudio Lab, Gammel Lundtoftevej 3B, Copenhagen, Denmark*
[2] *Dynaudio Lab, Gammel Lundtoftevej 3B, Copenhagen, Denmark*
[3] *Dynaudio Lab, Gammel Lundtoftevej 3B, Copenhagen, Denmark*

Correspondence should be addressed to Jianbin Yang (stanley.yang@goerdyna.com)

ABSTRACT
A dip has been often observed in loudspeaker frequency response, especially for loudspeakers with light surrounds. This study investigates the origin of the dip effect in the mid-range frequency by establishing a model of surround vibration. One design is proposed to lessen the dip effect, whose basic idea is to restrict surround displacement by delivering an additional air load resulting from air resonance in a closed cavity structure. The mechanism and effectiveness of the design are verified by simulation and experiment.

1 Introduction

The ideal frequency response of loudspeaker for sound reproduction is supposed to be a flat straight line [1]. However, a dip has been often observed in loudspeaker frequency response in the mid-range frequency [2], [3]. It is of great significance to eliminate the dip for loudspeaker design. Klippel proposed phase decomposition analysis for cone and surround based on a measured displacement pattern [4]. Christensen expanded the research to include COMSOL Multiphysics simulation [5]. Both of them, however, have not established a theoretical model describing surround vibration and revealed the relationship between the surround material property and dip effect.

This paper presents a model of surround vibration and analyzes the cause of dip in the loudspeaker mid-range frequency response. It then proposes one alternative design, that is, air cushion surround (ACS), to reduce the dip effect.

The structure of the paper is arranged as follows: Section 2 presents the surround vibration modeling. ACS is analyzed through theory and simulation in Section 3, and validated through experiment in Section 4. Finally, Section 5 provides the conclusions.

2 Surround Vibration modeling

Consider an ideal annular piston-like surround depicted in Fig. 1, under the following assumptions: (1) the inner edge $r = a$ of the surround is driven by the cone, while the outer edge $r = b$ is fixed. (2) The tension of the surround is constant and does not change with frequency. (3) The driving force is constant and steady. Therefore, the vibration equation of the surround is given by [6]

$$\frac{\partial^2 u}{\partial t^2} - C^2 \nabla^2 u = 0 \tag{1}$$

Internal use

where u is the vibration displacement, $C=\sqrt{T/\sigma}$, T is the tension per unit length, and σ is the mass per unit area.

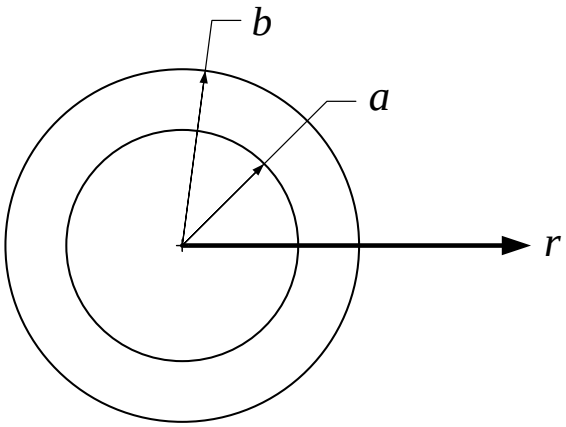


Figure 1. Top view of an annular piston-like surround.

The boundary conditions are given by

$$\begin{aligned} &u\big|_{r=b}=0 \\ &-T\left(2\pi r\frac{\partial u}{\partial r}\right)\Big|_{r=a}=Fe^{j\omega t} \end{aligned} \tag{2}$$

By replacing $u=\xi(r)e^{j\omega t}$ in Equation (1), the zero-order Bessel equation can be obtained as

$$\frac{d^2\xi}{\partial r^2}+\frac{1}{r}\frac{d\xi}{\partial r}+k^2\xi=0 \tag{3}$$

where $k=\omega/C$.

By combining Equation (2) and Equation (3), the surround amplitude $\xi(r)$ is given by [6]

$$\begin{aligned} &\xi(r)=\frac{F}{2\pi Tka}\times \\ &\left(\frac{J_0(kb)N_0(kr)-J_0(kr)N_0(kb)}{J_0(kb)N_1(ka)-J_1(ka)N_0(kb)}\right) \end{aligned} \tag{4}$$

where J_0, J_1 are the zero-order and first-order Bessel functions of the first kind, and N_0, N_1 are the zero-order and first-order Neumann functions.

For $0<kr\le 3$, based on the asymptotic formulations of $J_\nu(x)$ and $N_\nu(x)$ when $x\to 0$, $\nu=0,1$, Equation (4) may be approximated as [7–9]

$$\xi(r)\approx\frac{F}{2\pi T}\ln\frac{b}{r} \tag{5}$$

Consequently, Equation (5) shows that the amplitude of the surround in the low frequency region is simply connected to r and does not vary with frequency. The surround amplitude is largest on the inner boundary $r=a$ and drops with rising r until it reaches zero at $r=b$. Throughout this frequency range, it may be said that the surround and the cone vibrate in phase.

The surround and cone vibrations become less consistent as the frequency rises, and anti-resonance happens when the vibrations are out of phase. This explains how dip creation results from the cancelation of acoustic interference, leading to the appearance of a nodal circle at $r=a$ [7], [10]

$$\xi(r)\big|_{r=a}=0 \tag{6}$$

that is,

$$J_0(kb)N_0(kr)-J_0(kr)N_0(kb)=0 \tag{7}$$

Taking the first-order approximation yields the root of Equation (7) as [7], [9]

$$ka\approx\frac{\gamma_1\pi}{s-1} \tag{8}$$

where $\gamma_1=12.5$, $s=b/a$.

Replacing $k=\omega/C$ in Equation (8) yields

$$f_a\approx\frac{20}{a}\sqrt{\frac{T}{\sigma}} \tag{9}$$

which indicates that the anti-resonant frequency decreases with increasing mechanical compliance and surround density as the mechanical compliance C_f has the relationship of $C_f\sim 1/T$.

Similarly, replacing $k=\omega/C$ in Equation (4) yields

Internal use

$$\xi \sim \frac{\sqrt{C_f}}{\omega} \tag{10}$$

Consequently, it is evident that the surround amplitude increases with increasing C_f and decreasing frequency. Furthermore, when the anti-resonant frequency drops and the C_f rises, the dip in mid-range frequency response gets deeper. Thus, the dip effect will be improved if the stiffness of the surround is increased.

3 Theory and simulation of ACS

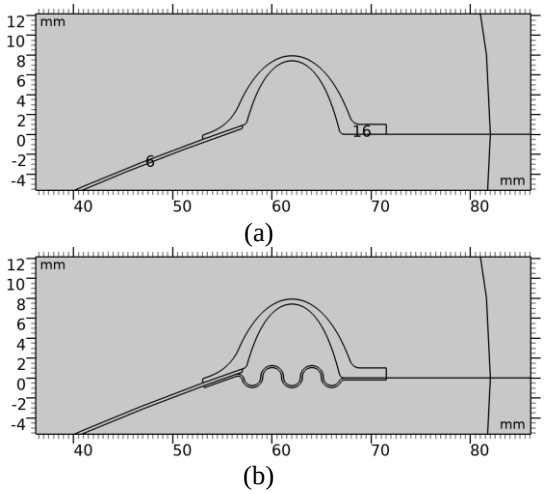


Figure 2. Comparison of (a) common surround and (b) air cushion surround.

According to the surround modeling in Section 2, to eliminate dips in the mid-range frequency response, the intuitive idea is to suppress the surround amplitude. This may explain several typical practices [7], including using high internal damping surround material, increasing the surround stiffness in accordance with Equation (10), decreasing the surround width in accordance with Equation (8), etc. The air cushion surround (ACS) design follows the same principle, with the addition of a cushion to create a closed cavity structure with the surround, as seen in Fig. 2. From the simulation based on the finite element method (FEM), the dip of loudspeaker driver's frequency response at 1400 Hz is reduced, as Fig. 3 illustrates.

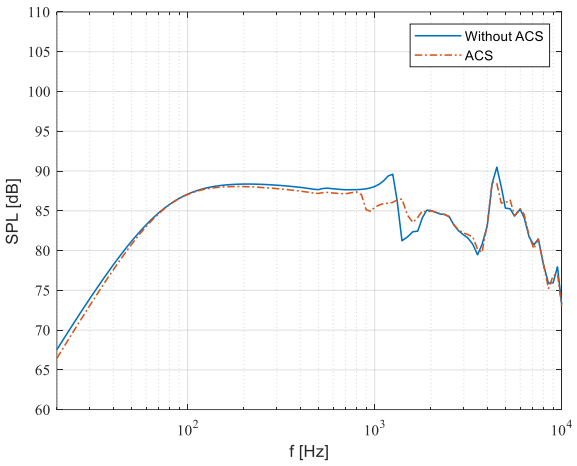


Figure 3. Comparison of simulated frequency responses of loudspeakers with or without ACS.

The basic concept of ACS, whose mechanism restricts surround displacement by delivering an additional air load resulting from air resonance in a closed cavity, is similar to that of passive-radiator loudspeakers [11–14]. The air in the cavity and the cushion suspension produces acoustic compliance, while the cushion provides the acoustic mass. The closed cavity air restricts the surround amplitude through the coupling resonance, as Fig. 4 illustrates.

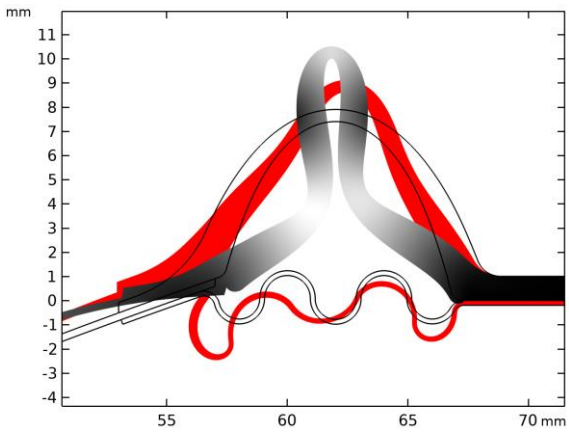


Figure 4. Loudspeaker driver surround displacement at 1400 Hz.

The closed-cavity resonance frequency f_s is defined as

$$f_s = \frac{1}{2\pi}\sqrt{\frac{K_{air}+K_c}{m_c}} \tag{11}$$

where m_c is mass of the cushion, and K_c is the effective mechanical stiffness of the cushion

Internal use

suspension. The effective mechanical stiffness of the closed cavity K_{air} is defined as

$$K_{air} = \frac{\rho_0 c_0^2 S_c^2}{V_{cavity}} \tag{12}$$

where V_{cavity} is the closed cavity volume, S_c is area of the cushion coupled to cavity, ρ_0 and c_0 are the air density and speed, respectively. FEM may be used to find the numerical solution of K_c, as Fig. 5 illustrates. Fig. 6 illustrates a closed-cavity resonance frequency curve with ACS density as the independent variable.

The theoretical resonant frequency of 1141 Hz is within the range of the ACS operating frequency range, as indicated by the simulation results in Fig. 3. The ACS operating frequency range is around 850 ~1700 Hz. The ACS operating frequency range can be reached by changing the cushion density ρ_c to 800 kg/m^3, 1000 kg/m^3, and 1400 kg/m^3, respectively. The corresponding cavity resonant frequencies are 1398 Hz, 1250 Hz, and 1057 Hz. The frequency responses get improved by the ACSs, as Fig. 7 illustrates. However, as Fig. 8 illustrates, the ACS performs poorly when the cushion density is adjusted to 482 kg/m^3, which corresponds to a closed-cavity resonance frequency of 1800 Hz that is outside the ACS operating frequency range. Moreover, the ACS fails when the cushion density drops to 100 kg/m^3 because the associated closed-cavity resonance frequency is farther outside of the ACS operating range.

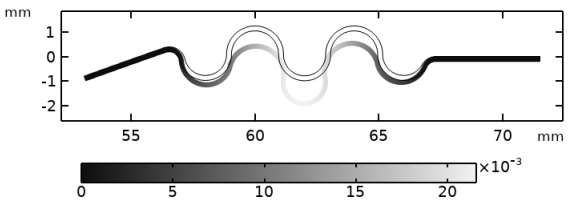


Figure 5. Simulation of K_c with FEM.

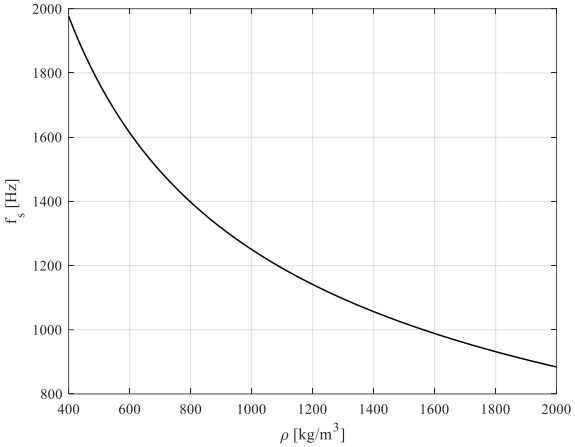


Figure 6. The resonant frequency f_s of the closed cavity of the ACS.

As seen in Fig. 9, a comparable circumstance also arises when the closed cavity volume varies. The equivalent closed cavity resonant frequencies, which fall within the operating frequency range of the ACS, are 1459 Hz and 1044 Hz, respectively, when the closed cavity volume is lowered by 40% or raised by 20%. For now, ACS contributes to better frequency response. The ACS fails when the associated closed cavity resonant frequency beyond the operating frequency range, which occurs when the closed cavity volume grows by 200%.

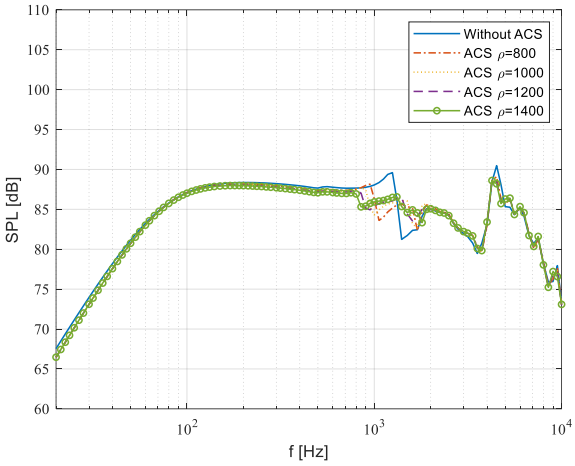


Figure 7. Comparison of simulated frequency responses of loudspeakers with different ρ_c that result in f_s falling inside the ACS's operating frequency range.

Internal use

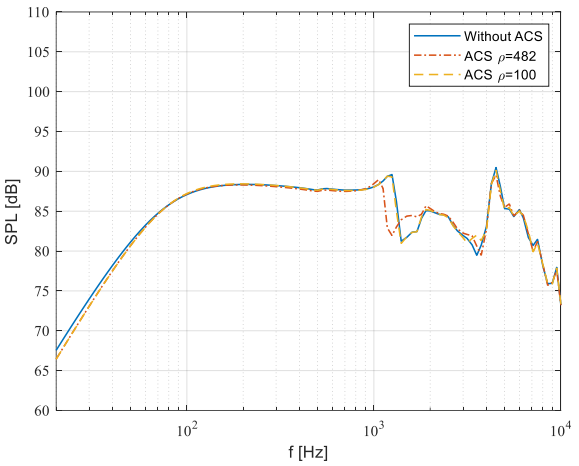


Figure 8. Comparison of simulated frequency responses of loudspeakers with different ρ_c that result in f_s beyond the ACS's operating frequency range.

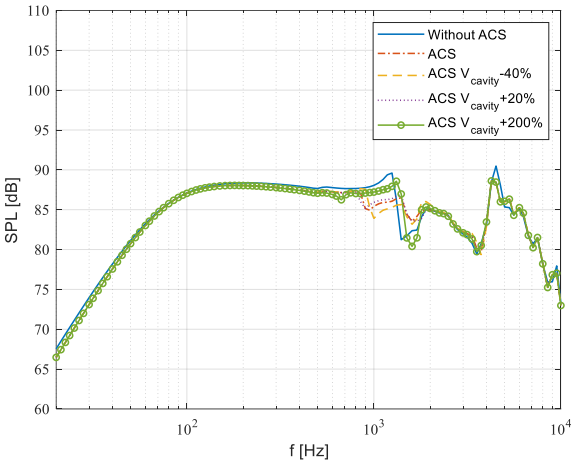


Figure 9. Comparison of simulated frequency responses of loudspeakers with various V_{cavity}.

It is important to note that the closed cavity construction that ACS developed is vital. As seen in Fig. 10, the surround density increases to 839 kg/m^3 from the initial 600 kg/m^3 if the mass of the cushion is added to the surround. However, this does little to improve the loudspeaker driver's frequency response dip effect. Besides, as Fig. 11 illustrates, when the cushion is drilled, the impact of ACS on improving frequency response diminishes as the cavity tightness weakens. It suggests that rather than only relying on the mass damping effect, the effect of ACS is highly dependent on the closed cavity.

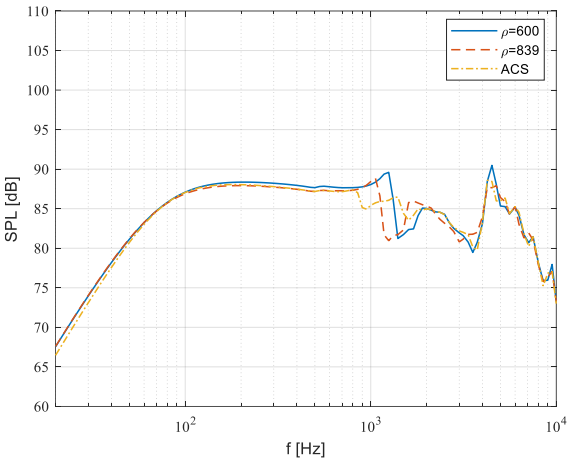


Figure 10. Comparison of simulated frequency responses between the loudspeakers with an equivalent surround or the original.

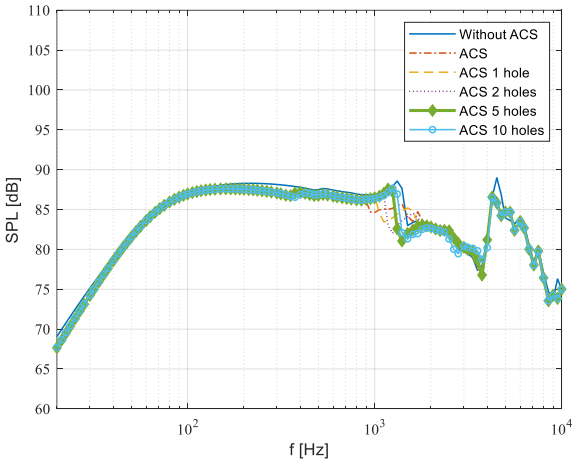


Figure 11. Comparison of simulated frequency responses of loudspeakers with cushion being drilled.

4 Experiment

To check the validity of ACS, experiments were carried out in a hemi-anechoic chamber. A Soundcheck analyzer (Listen, Inc.) generated a stepped sine signal in the range of 20 Hz to 20 kHz, which was sent to a 6.5-inch driver. A reference microphone (Type 4191, Brüel & Kjær) was placed in front of the driver with a measuring distance of 1 m. The experiment results shown in Fig. 12 demonstrate that ACS optimizes the loudspeaker driver's frequency response at 1~1.7 kHz, clearly suppresses the dip effect, and improves the curve's overall flatness. Besides, ACS mainly acts on the

Internal use

mid-range frequency response and has little effect on the low frequency response.

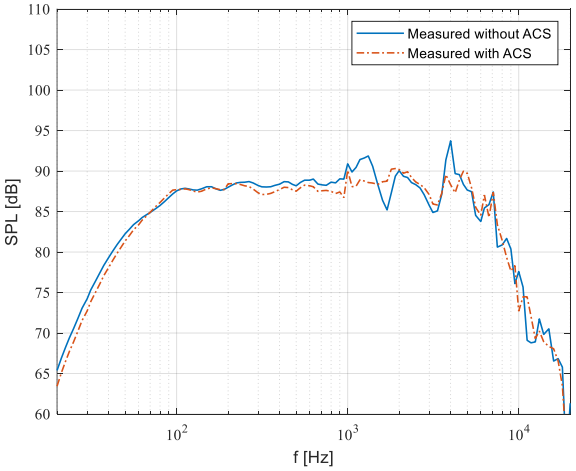


Figure 12. Comparison of measured frequency responses of loudspeakers with or without ACS.

5 Conclusions

This paper studies the cause of the dip effect in the loudspeaker driver's mid-range frequency response using surround modeling. The dip occurs from the out-of-phase vibrations of the cone and surround. It then suggests an ACS structural design to reduce the dip effect. In contrast to the conventional methods of directly optimizing surround, ACS reduces the anti-resonance effect between surround and cone by suppressing surround amplitude through the use of a closed cavity structure. Simulation demonstrates that its fundamental mechanism, which applies an extra air load arising from air resonance in a closed cavity, reduces surround displacement. Through experiment and simulation, the effectiveness of ACS is verified. The reduction of the dip effect by ACS improves frequency response, which is crucial for loudspeaker design.

References

[1] F. E. Toole, *Sound Reproduction: The Acoustics and Psychoacoustics of Loudspeakers and Rooms*, Focal Press (2008).

[2] H. F. Olson, J. Preston, and E. G. May, "Recent developments in direct radiator high-fidelity loudspeakers," *J. Audio Eng. Soc.*, vol. 2, pp.219—227 (1954).

[3] J. Eargle, *Loudspeaker Handbook*, 2nd ed, Kluwer, Boston (2003).

[4] W. Klippel, J. Schlechter, "Measurement and visualization of loudspeaker cone vibrations," presented at the *121st Convention of the Audio Engineering Society* (2006 Oct.).

[5] R. Christensen, "Phase Decomposition for Loudspeaker Analysis," in *Proceedings of the 2016 COMSOL Conference* in Munich (2016).

[6] J. Cheng, *The Principle of Acoustics*, Chinese ed, Science, Beijing (2012).

[7] S. Xu, H. Fan, "Holographic analysis of the squawker trough of the loudspeaker and the methods of improvement," *Journal of Nanjing University (Natural Science Edition)*, vol. 20, no. 4, pp. 665—674 (1984).

[8] E. T. Whittaker, *A course of modern analysis. An introduction to the general theory of infinite processes and of analytic functions: with an account of the principal transcendental functions*, Cambridge University Press, Printed in the USA (1962).

[9] M. Abramowitz, I. A. Stegun, *Handbook of mathematical functions with formulas, graphs, and mathematical tables*, US Government printing office (1968).

[10] F. J. M. Frankort, *Vibration and sound radiation of loudspeaker cones*, Eindhoven, Netherlands: NV Phillips' Gloeilampenfabrieken (1975).

[11] R. H. Small, "Passive-Radiator loudspeaker systems part I: Analysis," *J. Audio Eng. Soc.*, vol. 22, no. 8, pp. 592—601 (1974).

[12] R. H. Small, "Passive-Radiator loudspeaker systems part II: Synthesis," *J. Audio Eng. Soc.*, vol. 22, no. 9, pp. 683—689 (1974).

[13] T. L. Clarke, "Augmented Passive Radiator Loudspeaker Systems, Part I," *J. Audio Eng. Soc.*, vol. 29, no. 6, pp. 394—404 (1981).

[14] T. L. Clarke, "Augmented Passive Radiator Loudspeaker Systems, Part II," *J. Audio Eng. Soc.*, vol. 29, no. 7/8, pp. 511—516 (1981).